Available online at www.sciencedirect.com
ScienceDirect
Fluid Phase Equilibria 256 (2007) 34–41
FLUID PHASE EQUILIBRIA
www.elsevier.com/locate/fluid

Modeling acid–base equilibria and phase behavior in mixed-solvent electrolyte systems☆

Jerzy J. Kosinski, Peiming Wang, Ronald D. Springer, Andrzej Anderko*

OLI Systems, Inc., 108 American Road, Morris Plains, NJ 07950, USA

Received 21 September 2006; received in revised form 15 November 2006; accepted 22 November 2006
Available online 2 December 2006

Abstract

A comprehensive thermodynamic framework for mixed-solvent electrolyte systems has been applied to the simultaneous computation of phase behavior and acid–base equilibria. The computational approach combines an excess Gibbs energy model with a formulation for standard-state properties of individual species and an algorithm for speciation calculations. Using this framework, a consistent methodology has been established to calculate the pH of mixed-solvent solutions using a single, aqueous reference state. It has been shown that solid solubilities, vapor–liquid equilibria, solution pH and other properties can be reproduced for mixed solvents ranging from pure water to pure non-aqueous components and for solutes ranging from infinite dilution to the fused salt limit. In particular, the model has been shown to be accurate for mixtures containing hydrogen peroxide and ethylene glycol as solvents and various salts, acids and bases as solutes.

Keywords: Electrolytes; Solubility; Vapor–liquid equilibria; Speciation; pH

1. Introduction

Thermodynamic properties of electrolyte solutions result from a frequently complex interplay of electrostatic effects, short-range interactions and chemical equilibria between various ions and neutral species. A substantial number of electrolyte models have been reported in the literature and applied to the calculation of phase equilibria and other thermodynamic properties (cf. the reviews [1–5]). In a comprehensive electrolyte model, phase equilibrium computations need to be performed simultaneously with speciation calculations. Speciation, which results from chemical equilibria between solution species, is directly responsible for such important properties as pH, oxidation–reduction potential, and electrical conductivity. Also, there is a strong connection between phase equilibria and speciation effects such as acid–base equilibria and complexation. Such effects frequently play a key role in determining the solubilities of various solids and the volatility of species that may undergo chemical reactions in the liquid phase.

Although highly desirable from a practical point of view, inclusion of chemical equilibria in ionic systems poses some fundamental difficulties. While the properties of individual species and equilibrium constants are generally accessible for dilute solutions and many compilations of thermochemical data at infinite dilution are available, the distribution of individual species is typically poorly known in concentrated and, in particular, non-aqueous and mixed-solvent solutions. In the absence of specific spectroscopic data, it is frequently difficult to differentiate between the effects of chemical equilibria and "physical" non-ideality. Thus, the development of electrolyte models frequently needs to be guided by a compromise between the requirement to reproduce speciation-related properties (such as pH) and the practical tractability of a model in which chemical equilibria and solution non-ideality are intertwined.

In a previous study [6], a comprehensive model was developed for the computation of phase equilibria, speciation and other thermodynamic properties of electrolyte systems. This model was shown to be accurate for aqueous systems ranging from infinite dilution to the fused salt limit and for non-aqueous and mixed-solvent electrolyte systems. In a subsequent study

☆ Paper presented at the 16th Symposium on Thermophysical Properties, 30 July–4 August 2006, Boulder, CO, USA.

* Corresponding author. Tel.: +1 973 539 4996; fax: +1 973 539 5922.
E-mail address: aanderko@olisystems.com (A. Anderko).

0378-3812/$ – see front matter © 2006 Elsevier B.V. All rights reserved.
doi:10.1016/j.fluid.2006.11.018

[7], a methodology was developed for the practical treatment of proton solvation in concentrated strong acids and the model was shown to predict speciation in aqueous acid systems with good accuracy.

The objective of this work is to extend the previously developed thermodynamic model [6,7] to provide a simultaneous representation of acid–base equilibria and phase equilibria for systems that contain electrolytes in mixed solvents. For this purpose, a practical approach is proposed to calculate the pH of mixed-solvent system using a uniform reference state. Two practically important cases of hydrogen peroxide and monoethylene glycol as solvents are analyzed to validate the model.

2. Thermodynamic framework

The mixed-solvent electrolyte framework was described in detail in previous papers [6,7] and, therefore, only a brief summary is given here. The framework combines an excess Gibbs energy model for mixed-solvent electrolyte systems with a comprehensive treatment of chemical equilibria. The excess Gibbs energy is expressed as

$$\frac{G^{ex}}{RT} = \frac{G^{ex}_{LR}}{RT} + \frac{G^{ex}_{II}}{RT} + \frac{G^{ex}_{SR}}{RT} \tag{1}$$

where G^{ex}_{LR} represents the contribution of long-range electrostatic interactions, G^{ex}_{II} accounts for specific ionic (ion–ion and ion–molecule) interactions, and G^{ex}_{SR} is the short-range contribution resulting from intermolecular interactions. The long-range interaction contribution is calculated from the Pitzer–Debye–Hückel formula [8] expressed in terms of mole fractions and symmetrically normalized. The specific ion-interaction contribution is calculated from an ionic strength-dependent, symmetrical second virial coefficient-type expression [6]:

$$\frac{G^{ex}_{II}}{RT} = -\left(\sum_i n_i\right)\sum_i\sum_j x_i x_j B_{ij}(I_x) \tag{2}$$

where $B_{ij}(I_x) = B_{ji}(I_x)$, $B_{ii} = B_{jj} = 0$ and the ionic strength dependence of B_{ij} is given by

$$B_{ij}(I_x) = b_{ij} + c_{ij}\exp(-\sqrt{I_x + a_1}) \tag{3}$$

and where b_{ij} and c_{ij} are binary interaction parameters and a_1 is set equal to 0.01. In general, the parameters b_{ij} and c_{ij} are calculated as functions of temperature as

$$b_{ij} = b_{0,ij} + b_{1,ij}T + \frac{b_{2,ij}}{T} + b_{3,ij}T^2 + b_{4,ij}\ln T \tag{4}$$

$$c_{ij} = c_{0,ij} + c_{1,ij}T + \frac{c_{2,ij}}{T} + c_{3,ij}T^2 + c_{4,ij}\ln T \tag{5}$$

The last two parameters of Eqs. (4) and (5) are typically necessary only when there is a need to reproduce experimental data over a very wide range of temperatures, e.g., from −50 to 300 °C.

The short-range interaction contribution is calculated from the UNIQUAC equation [9]. When justified by experimental data, the temperature dependence of the UNIQUAC energetic parameters can be expressed using a function that extends up to the quadratic term, i.e.,

$$a_{ij} = a^{(0)}_{ij} + a^{(1)}_{ij}T + a^{(2)}_{ij}T^2 \tag{6}$$

In systems containing only strong electrolytes, the specific ion-interaction parameters are the only parameters that need to be determined to reproduce the properties of the solution. In purely non-electrolyte systems, only the short-range parameters are needed. In the case of weak electrolytes or mixed electrolyte–non-electrolyte systems, the mixture is characterized by a certain combination of the specific ion-interaction and short-range interaction parameters.

While the excess Gibbs energy model is used to calculate non-ideality effects, chemical equilibrium computations require the use of standard-state chemical potentials of individual species, $\mu^0_i(T, P)$, in addition to their activity coefficients, $\gamma_i(T, P, x)$, i.e.,

$$\mu_i(T, P, x) = \mu^0_i(T, P) + RT\ln x_i\gamma_i(T, P, x) \tag{7}$$

The standard-state chemical potentials for aqueous species, $\mu^0_i(T, P)$, are calculated as functions of temperature and pressure using the Helgeson–Kirkham–Flowers–Tanger (HKFT) equation of state [10,11]. The excess Gibbs energy model is made consistent with the HKFT equation by (i) converting the activity coefficients calculated from Eq. (1) to those based on the unsymmetrical reference state, i.e. at infinite dilution in water and (ii) converting the molality-based standard-state chemical potentials to corresponding mole fraction-based quantities [6]. For speciation calculations in organic or mixed-solvent electrolyte solutions, the chemical potential of the species is modeled by combining aqueous standard-state properties with available Gibbs energies of transfer. This is achieved by constraining the activity coefficient model parameters so that the Gibbs energy of transfer of ions from water to a non-aqueous solvent can be reproduced [6].

3. Treatment of acid–base equilibria

The pH of a solution is an experimentally accessible and practically important reflection of acid–base equilibria. Although several practical definitions of pH have been used in the literature, the most commonly used definition [15] is based on the activity of H^+ ions in molality units, i.e.,

$$\mathrm{pH} = -\log a_{H^+} = -\log\left(\frac{m_{H^+}\gamma^m_{H^+}}{m^0}\right) \tag{8a}$$

where m^0 is a unit molality (1 mol/kg solvent) and the activity coefficient $\gamma^m_{H^+}$ is based on the molality scale and is unsymmetrically normalized, i.e., it reaches 1 at infinite dilution in a given solvent. An alternative definition is based on molarity units, i.e.,

$$\mathrm{pH} = -\log a_{H^+} = -\log\left(\frac{C_{H^+}\gamma^c_{H^+}}{C^0}\right) \tag{8b}$$

This definition of pH applies to any solvent. However, the values of pH in various solvents calculated from Eqs. (8a) and (8b) are solvent-specific and are not necessarily directly comparable

because the reference state for the activity of H^+ is different for each solvent. In principle, the pH scales in different solvents may be interrelated by using the Gibbs energy of transfer of the H^+ ions. The Gibbs energy of transfer is the difference between the chemical potential of H^+ at infinite dilution in water and in a different solvent. Accordingly, the chemical potential of H^+ in an aqueous solution with a given value of pH_w is equal to the chemical potential of H^+ in a solvent A, in which the pH is given by

$$pH_A = pH_w + \frac{\Delta G^{t,w\to A}_{H^+}}{RT \ln 10} \tag{9}$$

where $\Delta G^{t,w\to A}_{H^+}$ is the Gibbs energy of transfer from water to solvent A. This relationship opens the possibility of using just one, aqueous, reference state for practical calculations. However, the direct usefulness of Eq. (9) is limited by the availability of Gibbs energies of transfer and by the inherent necessity of making extra-thermodynamic assumptions to separate the Gibbs energy of transfer into the contributions of cations and anions [16]. Nevertheless, a comprehensive thermodynamic model can be expected to yield reasonable values of pH with a uniform, water-based reference state as long as the model is capable of reproducing the activity coefficients of individual species and the Gibbs energy of transfer [6].

Since the model used in this work is defined in terms of mole fractions, Eq. (8a) needs to be rewritten as

$$pH = -\log x_{H^+} - \log \gamma^x_{H^+} - \log\left(\frac{1000}{M_{H_2O}}\right) \tag{10}$$

where the activity coefficient is defined on the mole fraction scale and the last term converts the activity from the molality to the mole fraction scale. Further, it has been demonstrated in a previous paper [7] that it is advantageous to consider protons as solvated entities (e.g., H_3O^+) for modeling the properties of acids. In a treatment that explicitly recognizes solvated protons, the standard-state properties of the hydronium ion are additive with respect to its two constituent entities, i.e., H^+ and H_2O. This is due to the fact that the H_3O^+ ion at infinite dilution in H_2O is indistinguishable from an entity consisting of the two constituent species, H^+ and H_2O. Therefore, the standard-state chemical potentials of H_3O^+, H^+ and H_2O satisfy the relationship $\mu^0_{H_3O^+} = \mu^0_{H^+} + \mu^0_{H_2O}$ at all temperatures and pressures. Subsequently, the equality of chemical potentials for the reaction $H_3O^+ = H^+ + H_2O$ requires that $a_{H_3O^+} = a_{H^+}a_{H_2O}$ and Eq. (10) becomes

$$pH = -\log x_{H_3O^+} - \log \gamma^x_{H_3O^+} - \log\left(\frac{1000}{M_{H_2O}}\right) + \log x_{H_2O} + \log \gamma^x_{H_2O}. \tag{11}$$

Eq. (11) can be easily generalized to solvents other than water. In a protic solvent HA, protons can be solvated as H_2A^+. Assuming that the equilibrium constant of the reaction:

$$H_3O^+{}_{aq} + HA_{aq} = H_2O_{aq} + H_2A^+{}_{aq} \tag{12}$$

is $K_{H_2A^+}$, Eq. (11) becomes equivalent to

$$pH = \log K_{H_2A^+} - \log x_{H_2A^+} - \log \gamma^x_{H_2A^+} - \log\left(\frac{1000}{M_{H_2O}}\right) + \log x_{HA} + \log \gamma^x_{HA} \tag{13}$$

and does not require the presence of water in the system.

In practice, the pH calculated from the model can be used in one of two alternative ways:

(i) The value of pH can be calculated directly from the general equation (11). In this case, pH is always consistent with the generalized water-based reference scale.
(ii) It can be recalculated using a solvent-specific scale. This may be useful if experimental data are reported on a solvent-specific basis. For this purpose, it can be assumed that the pH value for a fairly dilute strong acid solution in a given solvent is fixed at a certain value. For example, such a value may be assumed equal to the pH of a hypothetical aqueous solution at the same concentration of the acid [19]. Then, the difference between the pH value calculated from Eq. (11) and the assumed value constitutes a correction that can be used for the translation of the pH scale.

4. Results and discussion

In this study, we apply the formalism outlined above to systems containing electrolytes in mixed H_2O_2–H_2O and glycol–H_2O systems. For H_2O_2–H_2O solutions, acid–base equilibria take the form:

$$H_2O_2 + H_2O = H_3O^+ + HO_2^- \tag{14}$$

and

$$2H_2O_2 = H_3O_2^+ + HO_2^- \tag{15}$$

Since H_2O_2 is somewhat more acidic than H_2O, reaction (14) dominates in solutions, especially in the H_2O-rich regions. Eq. (15) is significant only in pure H_2O_2 and concentrated solutions. Since thermochemical properties of ions are available mostly from aqueous solution data, the properties of the HO_2^- ions are known with a much better accuracy than those of $H_3O_2^+$. Consequently, the Gibbs energy of formation of $H_3O_2^+$ has been treated as an adjustable parameter in this study whereas the entropy of $H_3O_2^+$ has been taken from Evans and Uri [17]. For the HO_2^- ion, literature data have been used [17]. To develop model parameters for systems containing H_2O_2, data of several types have been used, i.e.,

(i) Vapor–liquid equilibria, heat capacities and densities of H_2O_2–H_2O mixtures. These data are used to determine the short-range (UNIQUAC) binary parameters between H_2O_2 and H_2O. Data of this kind are not sensitive to ionization.
(ii) pH measurements for NaOH, H_2SO_4 and $HClO_4$ in H_2O_2–H_2O mixtures [18,19], which were obtained using glass electrodes without employing reference solutions to recalculate the obtained pH to conform with a solvent-specific pH scale. Assuming that the glass electrode does

not change its characteristics with a change in solvent composition, the apparent pH values obtained in this way should be consistent with Eq. (11). In most cases, this assumption cannot be independently verified through experimentation. However, the electrode response is primarily determined by the activity of solvated protons, which is, in turn, influenced by solvent composition. While the validity of this assumption cannot be proven, it can be indirectly confirmed if a consistent treatment of pH can be obtained for various solutes and solvent compositions. The effect of the change in solvent composition on pH is then accounted for by the change in activity coefficients of H_3O^+ and H_2O. To reproduce this kind of data, temperature-independent specific ion-interaction parameters have been determined for the H_2O_2–HO_2^-, H_2O_2–H_3O^+ and H_2O–HO_2^- ion pairs in addition to adjusting the Gibbs energy of formation of the $H_3O_2^+$ ion. These parameters are independent of the particular solute (acid or base). Prior to determining these parameters, the fundamental parameters for aqueous solutions of acids and bases were determined as described in previous papers [6,7].

(iii) pH measurements obtained using glass electrodes that were calibrated (e.g., using perchloric acid) for each solution composition [19–21]. The pH value of a pure mixed solvent is determined in such measurements from the equivalence point that results from the neutralization of a dilute strong acid with a strong base. In such a solvent-specific pH scale, the experimental pH can be approximately identified with values calculated using the traditional molarity-based definition of pH (i.e., $pH = -\log C_{H^+}$), after taking into account that protons may exist in more than one solvated state, i.e.,

$$pH_{corrected} \approx -\log C_{H^+,total} = -\log(C_{H_3O^+} + C_{H_3O_2^+}) \quad (16)$$

This expression is an approximate form of Eq. (8b), in which the activity coefficients are assumed to be equal to 1 as long as the ions are very dilute. It should be noted that Eq. (16) does not have the general character of Eq. (11). Rather, it approximately reflects the conditions of the experimental titration measurements for H_2O_2, in which the acidic species in various solvated forms are neutralized with a strong base. Thus, the measured "corrected" pH approximately corresponds to the total concentration of acidic species in a dilute solution. The data of this kind are used in conjunction with the apparent pH values (cf. (ii)) in the regression of the specific ion-interaction parameters.

Tables 1 and 2 summarize the parameters for the aqueous systems that were modeled in this study. Table 1 identifies all individual, ionic or neutral, species that have been assumed for the calculations reported here. Further, it lists the parameters that are necessary for each species, i.e., the standard-state Gibbs energy of formation, entropy, parameters of the HKFT equation of state and van der Waals volumes and surface areas. As shown in Table 1, the model assumes the presence of base inorganic ions for which well-defined thermochemical properties are available in the literature (i.e., OH^-, Na^+, NO_3^-, Cl^-, ClO_4^-, HO_2^-), hydrated protons in aqueous environments (H_3O^+), an ion pair with well-defined properties ($NaOH_{(aq)}$), neutral species whose properties can be derived from VLE and calorimetric data (i.e., $H_2O_{2(aq)}$, ethylene glycol $C_2H_6O_{2(aq)}$) and ions that result from the ionization of solvents (i.e., $H_3O_2^+$, ethylene glycolate $C_2H_5O_2^-$, ethylene glycoxonium $C_2H_7O_2^+$). As described in a previous paper [7], the proton is assumed to be solvated with the formation of H_3O^+ ions and its analogs in hydrogen peroxide ($H_3O_2^+$) and ethylene glycol ($C_2H_7O_2^+$).

For the common ions of interest, the standard-state properties and HKFT coefficients were taken from Shock and Helgeson [12] and Shock et al. [13]. For the H_3O^+ ion, these parameters were regressed to satisfy the requirement that the standard Gibbs energy change for the formation reaction $H_3O^+ = H^+ + H_2O$ equals zero at temperatures up to 500 °C and pressures up to 1 kbar. This requirement follows from the fact that the H_3O^+ ion at infinite dilution in H_2O is indistinguishable from an entity consisting of the two constituent species, H^+ and H_2O. The prop-

Table 1
Parameters for individual ionic and neutral species: Gibbs energy of formation, entropy, parameters of the Helgeson–Kirkham–Flowers [10–13] equation of state for standard partial molar thermodynamic properties ($a_{HKF,1,\ldots,4}$, $c_{HKF,1}$, $c_{HKF,2}$, ω) and van der Waals volume and surface area parameters in the UNIQUAC term

Species	$\Delta\overline{G}_f^\circ$ (kJ mol^{-1})	$\overline{S}^\circ$ (J mol^{-1} K^{-1})	$a_{HKF,1}$	$a_{HKF,2}$	$a_{HKF,3}$	$a_{HKF,4}$	$c_{HKF,1}$	$c_{HKF,2}$	ω	r	q
OH^- [a]	−157.298	−10.711	0.12527	7.38	1.8423	−27821	4.15	−103460	172460	0.92	1.4
H_3O^+ [b]	−237.175	69.994	0.45123	−21.2711	−8.64735	20487.1	14.6773	16975.9	−13672.5	0.92	1.4
Na^+ [a]	−261.881	58.4086	0.1839	−228.5	3.256	−27260	18.18	−29810	33060	0.92	1.4
NO_3^- [a]	−110.905	146.942	0.73161	678.24	−4.6838	−30594	7.7	−67250	109770	0.92	1.4
Cl^- [a]	−131.290	56.735	0.4032	480.1	5.563	−28470	−4.4	−57140	145600	0.92	1.4
ClO_4^- [a]	−8.535	182.004	0.81411	1730.6	−12.225	−34944	22.3	−89000	96990	0.92	1.4
HO_2^- [b]	−67.362	23.788	0.26566	−129.61	6.2619	−27253	−1.519	−106529	154490	1.196	1.809
$H_3O_2^+$ [b]	−74.842	121.369								1.196	1.809
$C_2H_5O_2^-$ [b]	−252.006	145.397								1	1
$C_2H_7O_2^+$ [b]	−317.368	254.2								1	1
$NaOH_{(aq)}$ [a]	−358.437	242.669	0.22338	−232.87	6.668	−26826	4.0146	−36863	−3000	0.92	1.4
$H_2O_{2(aq)}$ [c]	−133.587	121.369								1.196	1.809
$C_2H_6O_{2(aq)}$ [b]	−334.660	248.97					−0.60938	94768	97218	2.409	2.409

The formulas $C_2H_5O_2^-$, $C_2H_7O_2^+$ and $C_2H_6O_2$ denote the ethylene glycolate ion, ethylene glycoxonium ion and ethylene glycol, respectively.

[a] Standard-state properties were obtained from Refs. [12,13].

[b] Standard-state properties were determined in this study.

[c] Standard-state heat capacity and density are calculated from pure-component heat capacity and density as described in a previous paper [6].

Table 2
Binary parameters for the systems investigated in this study

Species i	Species j	$b_{0,ij}$	$b_{1,ij}$	$b_{2,ij}$	$b_{3,ij}$	$b_{4,ij}$	$c_{0,ij}$	$c_{1,ij}$	$c_{2,ij}$	$c_{3,ij}$	$c_{4,ij}$
Parameters of the ionic interaction term (Eqs. (4) and (5))											
Cl^-	Na^+	15611	7.9642	−357990	−0.0036431	−2892.7	−30086	−15.010	699850	0.0068210	5552.3
NO_3^-	Na^+	252.54	−0.46165	−42982	0.00023981	0	−383.93	0.60763	70566	−0.0001939	0
OH^-	Na^+	215.83	−0.26000	−51254	0	0	−395.22	0.51143	85055	0	0
H_2O_2	H_3O^+	−4.4148	0	0	0	0	0	0	0	0	0
H_2O_2	HO_2^-	1.43792	0	0	0	0	0	0	0	0	0
H_2O_2	Na^+	−10.334	0.016456	1544.93	0	0	0	0	0	0	0
H_2O_2	NO_3^-	−10.334	0.016456	1544.93	0	0	0	0	0	0	0
NaOH	H_2O	2.1987	0.0034304	0	0	0	−1.3065	−0.002641	0	0	0
$C_2H_6O_2$	Na^+	−1.8859	0	641.54	0	0	0	0	0	0	0

Species i	Species j	$a_{ij}^{(0)}$	$a_{ji}^{(0)}$	$a_{ij}^{(1)}$	$a_{ji}^{(1)}$	$a_{ij}^{(2)}$	$a_{ji}^{(2)}$
Parameters of the UNIQUAC term (Eq. (6))							
H_2O_2	HO_2^-	3522	10,000	0	0	0	0
H_2O	H_2O_2	−3560	1,995	14.585	−26.359	−0.028033	0.064409
H_2O_2	HO_2^-	10686	10,000	0	0	0	0
$C_2H_6O_2$	H_2O	26.38	31,272	−7.2411	−169.22	−0.0014349	0.24911
$C_2H_6O_2$	Na^+	325.2	11,871	0	0	0	0
Cl^-	$C_2H_6O_2$	4696	1,717	0	0	0	0

erties of H_2O were calculated from the Haar–Gallagher–Kerr equation of state [14] at all temperatures and pressures. The standard-state properties of other species in Table 1 were calculated to ensure agreement with (i) experimental Henry's law constants, (ii) experimental equilibrium constants for ionization and (iii) the previously determined standard-state properties of base ions that participate in dissociation reactions. It should be noted that the HKFT parameters could not be determined for some species for which experimental data were very limited. In such cases, only the Gibbs energy of formation and entropy are reported in Table 1. Table 2 summarizes the binary parameters that have been determined for the ion-interaction term (Eqs. (4) and (5)) and the UNIQUAC term (Eq. (6)).

Figs. 1–5 show the results of calculations for neutral, acidic and basic H_2O_2 solutions. Fig. 1 compares the calculated and experimental [22] vapor–liquid equilibria. While VLE is not sensitive to ionization in this case, the agreement with experimental data validates the accuracy of activities for neutral species. Fig. 2

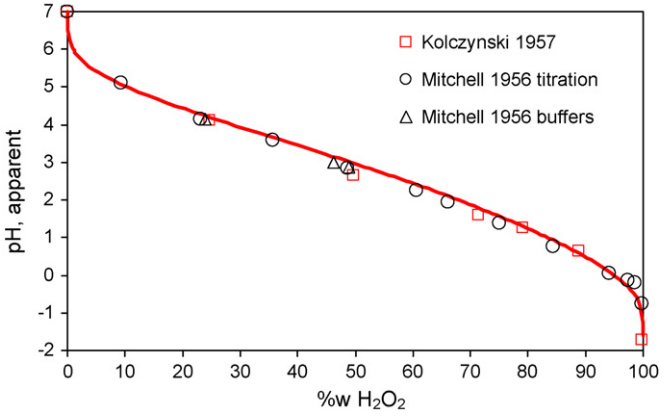

Fig. 2. Calculated and experimental [19,21] apparent pH for the system H_2O_2–H_2O.

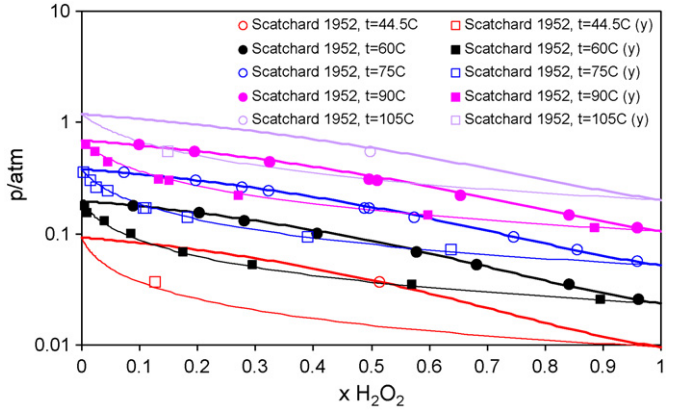

Fig. 1. Calculated and experimental [22] vapor–liquid equilibria for the system H_2O_2–H_2O.

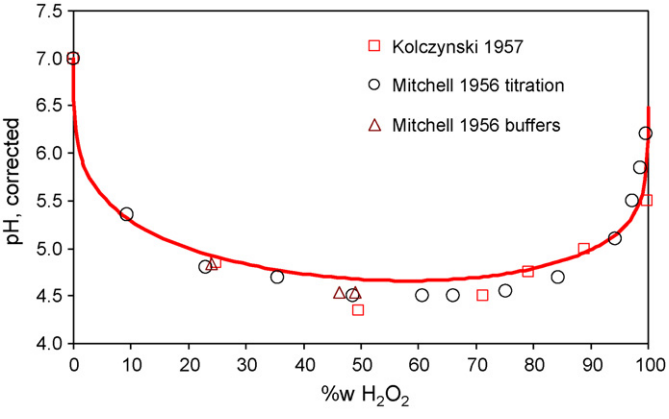

Fig. 3. Calculated and experimental [19,21] "corrected" pH for the system H_2O_2–H_2O.

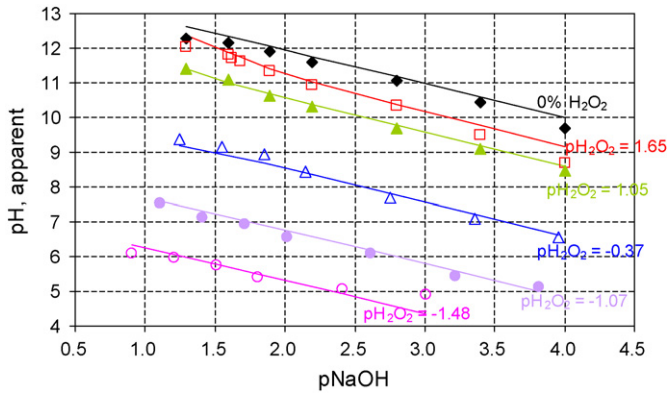

Fig. 4. Calculated and experimental [18] apparent pH of NaOH in H_2O_2–H_2O solvents.

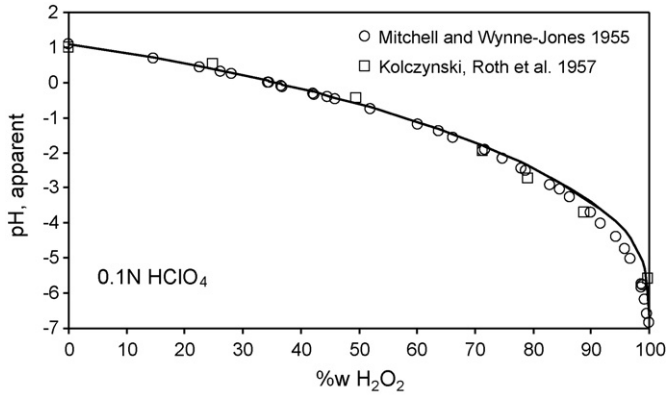

Fig. 5. Calculated and experimental [19,20] apparent pH of 0.1N $HClO_4$ solutions in mixed H_2O_2–H_2O solvents.

shows the apparent pH (Eq. (11)) of the system H_2O_2–H_2O as a function of composition. Fig. 3 shows the same dependence using a "corrected" pH scale (Eq. (16)). Fig. 4 illustrates the effect of solvent composition on the apparent pH of NaOH solutions. In this figure, concentration of the base is defined on a molarity basis as $pNaOH = -\log C_{NaOH}$. The calculated values are nearly linear as a function of pNaOH and agree with the data essentially within experimental scattering. Some deviations are observed for higher pNaOH values, but they do not have a systematic character when lines for different pH_2O_2 values are compared. Fig. 5 shows the variation of apparent pH with solvent composition for $HClO_4$ solutions. In all cases, the experimental pH values are correctly reproduced.

The effect of solvent composition on the solubility of solids is of particular interest. In this study, the effect of solvent composition on the solubility of $NaNO_3$ and NaCl has been investigated.

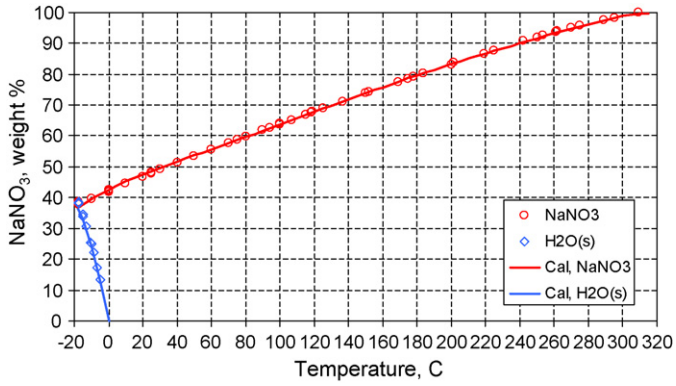

Fig. 6. Calculated and experimental [23] solid–liquid equilibria in the system $NaNO_3$–H_2O.

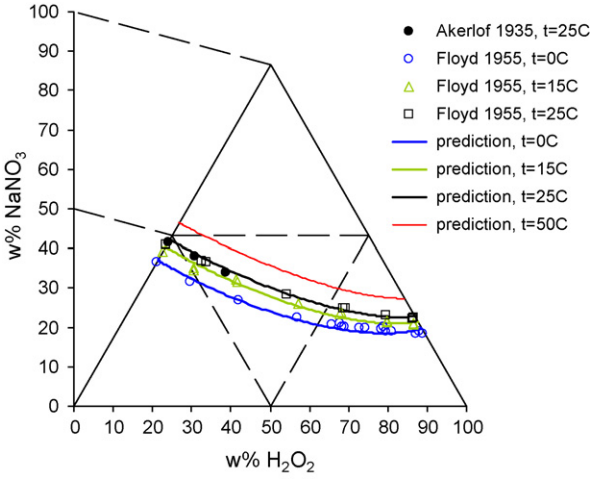

Fig. 7. Calculated and experimental [24,25] solubilities in the system $NaNO_3$–H_2O_2–H_2O.

Table 3 summarizes the thermochemical parameters of solid phases that are necessary to compute the chemical potential of the solid phase as a function of temperature according to standard thermodynamic relations. Then, solid–liquid equilibria can be calculated by equating the chemical potential of the solid phase with the sum of the chemical potentials of the dissolved species [3].

Fig. 6 shows a solid–liquid equilibrium phase diagram for the binary system $NaNO_3$–H_2O, for which extensive experimental data are available [23]. It is noteworthy that the model reproduces the solubility data from −20 °C up to the fused salt limit at ∼309 °C. In Fig. 7, the model is applied to the ternary system $NaNO_3$–H_2O–H_2O_2, for which experimental data are available only over a limited temperature range [24,25].

Table 3
Gibbs energy of formation, entropy and heat capacity coefficients for solid phases

Solid phase	$\Delta\overline{G}^\circ_f$ (kJ mol^{-1})	S° (J mol^{-1} K^{-1})	C_p (J mol^{-1} K^{-1}) $= A + B/T + C/T^2 + DT^2 + ET^3$				
			A	B	C	D	E
$NaNO_3$(s)	−366.106	119.713	−493.9911	4.577221	0	−0.011965	1.0789e−05
NaCl(s)	−384.324	70.7640	47.121	0.007219	20900	1.1156e−05	0
NaCl·2H_2O(s)	−858.845	164.613	130.1224	0	0	0	0

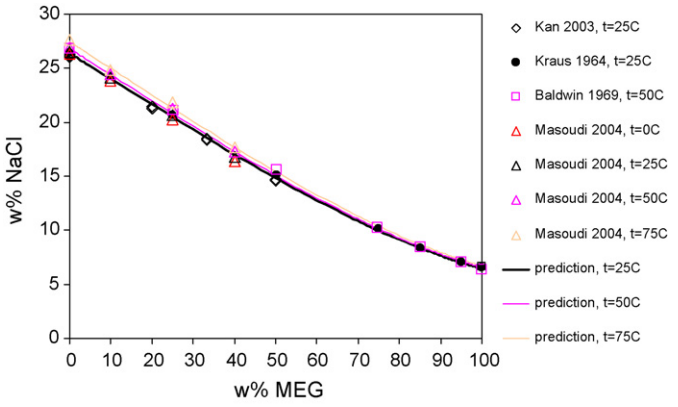

Fig. 8. Calculated and experimental [26–29] solubilities of NaCl in monoethylene glycol–water solutions.

The model represents the solubility data within experimental error.

The formalism described in this paper is not limited to hydrogen peroxide solutions and is applicable to a wide variety of protic solvents. Fig. 8 illustrates solubility calculations for a system containing monoethylene glycol (MEG), sodium chloride and water. The parameters for this system are also included in Tables 1–3. It should be noted that these parameters have also been verified for other systems containing chloride and sodium ions in MEG–H_2O solvents. As shown in Fig. 8, the model reproduces the solubility of NaCl in MEG–H_2O solutions with good accuracy. While the solubility strongly depends on solvent composition, it is very weakly affected by temperature.

5. Conclusions

A comprehensive thermodynamic model for mixed-solvent electrolyte systems has been applied to mixtures containing H_2O_2, monoethylene glycol and inorganic acids, bases and salts. It has been shown that the model can simultaneously represent phase equilibria and solution pH for solvents ranging from pure water to pure H_2O_2 and for solutes ranging from infinitely dilute to the pure solute or fused salt limit.

List of symbols

a_i activity of component i
a_{ij} temperature-dependent binary parameter in the UNIQUAC term
$a_{ij}^{(k)}$ kth constant in the temperature dependence of the UNIQUAC term (Eq. (6))
$a_{\mathrm{HKF},k}$ kth ($k=1, \ldots, 4$) volumetric parameter in the Helgeson–Kirkham–Flowers equation
b_{ij} temperature-dependent coefficient of the ionic interaction term $G_{\mathrm{II}}^{\mathrm{ex}}$ (Eq. (3))
$b_{k,ij}$ kth constant in the temperature dependence of the parameter b_{ij} (Eq. (4))
B_{ij} ionic strength and temperature-dependent virial coefficient in $G_{\mathrm{II}}^{\mathrm{ex}}$
c_{ij} temperature-dependent coefficient of the ionic interaction term $G_{\mathrm{II}}^{\mathrm{ex}}$ (Eq. (3))
$c_{k,ij}$ kth constant in the temperature dependence of the parameter c_{ij} (Eq. (5))
$c_{\mathrm{HKF},k}$ kth ($k=1, 2$) heat capacity-related parameter in the Helgeson–Kirkham–Flowers equation
C_i molarity of component i
C_p heat capacity
G^{ex} excess Gibbs energy
$G_{\mathrm{II}}^{\mathrm{ex}}$ ionic interaction contribution to the excess Gibbs energy
$G_{\mathrm{LR}}^{\mathrm{ex}}$ long-range interaction contribution to the excess Gibbs energy
$G_{\mathrm{SR}}^{\mathrm{ex}}$ short-range interaction contribution to the excess Gibbs energy
$\Delta G_{\mathrm{f}}^{\circ}$ standard Gibbs energy of formation
$\Delta \overline{G}_{\mathrm{f}}^{\circ}$ standard partial molar Gibbs energy of formation
$\Delta G_i^{\mathrm{t,w}\rightarrow\mathrm{A}}$ Gibbs energy of transfer of species i from solvent w to A
I_x mole fraction-based ionic strength
K equilibrium constant
m_i molality of component i
m^0 unit molality (1 mol/kg H_2O)
M molecular weight
$\mathrm{pH_A}$ pH expressed in a scale defined for solvent A
q van der Waals surface area parameter in the UNIQUAC term
r van der Waals volume parameter in the UNIQUAC term
R gas constant
S° entropy of a pure component
$\overline{S}^{\circ}$ partial molar entropy
T temperature
x_i mole fraction of component i

Greek symbols

γ_i activity coefficient of component i
γ_i^{m} activity coefficient of component i on a molality basis
γ_i^{x} activity coefficient of component i on a mole fraction basis
μ_i chemical potential of component i
μ_i^0 standard-state chemical potential of component i
ω parameter in the Helgeson–Kirkham–Flowers equation

Acknowledgment

This work was supported by Alcoa, Chevron, DuPont, Mitsubishi Chemical, Rohm&Haas and Shell.

References

[1] J.F. Zemaitis Jr., D.M. Clark, M. Rafal, N.C. Scrivner, Handbook of Aqueous Electrolyte Thermodynamics, DIPPR, AIChE, New York, 1986.
[2] K.S. Pitzer (Ed.), Activity Coefficients in Electrolyte Solutions, 2nd ed., CRC Press, 1991.
[3] M. Rafal, J.W. Berthold, N.C. Scrivner, S.L. Grise, in: S.I. Sandler (Ed.), Models for Thermodynamic and Phase Equilibria Calculations, Marcel Dekker, New York, 1994, pp. 601–670.
[4] J.R. Loehe, M.D. Donohue, AIChE J. 43 (1997) 180–195.
[5] A. Anderko, P. Wang, M. Rafal, Fluid Phase Equilib. 194/197 (2002) 123–142.

[6] P. Wang, A. Anderko, R.D. Young, Fluid Phase Equilib. 203 (2002) 141–176.
[7] P. Wang, A. Anderko, R.D. Springer, R.D. Young, J. Mol. Liquids 125 (2006) 37–44.
[8] K.S. Pitzer, J. Am. Chem. Soc. 102 (1980) 2902–2906.
[9] D.S. Abrams, J.M. Prausnitz, AIChE J. 21 (1975) 116–128.
[10] H.C. Helgeson, D.H. Kirkham, G.C. Flowers, Am. J. Sci. 274 (1974) 1089–1198;
H.C. Helgeson, D.H. Kirkham, G.C. Flowers, Am. J. Sci. 274 (1974) 1199–1261;
H.C. Helgeson, D.H. Kirkham, G.C. Flowers, Am. J. Sci. 276 (1976) 97–240;
H.C. Helgeson, D.H. Kirkham, G.C. Flowers, Am. J. Sci. 281 (1981) 1241–1516.
[11] J.C. Tanger, H.C. Helgeson, Am. J. Sci. 288 (1988) 19–98.
[12] E.L. Shock, H.C. Helgeson, Geochim. Cosmochim. Acta 52 (1988) 2009–2036.
[13] E.L. Shock, D.C. Sassani, M. Willis, D.A. Sverjensky, Geochim. Cosmochim. Acta 61 (1997) 907–950.
[14] L. Haar, J.S. Gallagher, G.S. Kell, NBS/NRC Steam Tables: Thermodynamic and Transport Properties and Computer Programs for Vapor and Liquid States of Water in SI Units, Hemisphere Publications, 1994.
[15] R.P. Buck, S. Rondinini, A.K. Covington, F.G.K. Baucke, C.M.A. Brett, M.F. Camoes, M.J.T. Milton, T. Mussini, R. Naumann, K.W. Pratt, P. Spitzer, G.S. Wilson, Pure Appl. Chem. 74 (2002) 2169–2200.
[16] Y. Marcus, Pure Appl. Chem. 58 (1986) 1721–1736.
[17] M.G. Evans, N. Uri, Trans. Faraday Soc. 45 (1949) 224–230.
[18] J.S. Reichert, H.G. Hull, Ind. Eng. Chem. Anal. Ed. 11 (1939) 311–314.
[19] J.R. Kolczynski, E.M. Roth, E.S. Shanley, J. Am. Chem. Soc. 79 (1957) 531–533.
[20] A.G. Mitchell, W.F.K. Wynne-Jones, Trans. Faraday Soc. 51 (1955) 1690–1697.
[21] A.G. Mitchell, W.F.K. Wynne-Jones, Trans. Faraday Soc. 52 (1956) 824–830.
[22] G. Scatchard, G.M. Kavanagh, L.B. Ticknor, J. Am. Chem. Soc. 74 (1952) 3715–3720.
[23] W.F. Linke, A.S. Seidell, Solubilities of Inorganic and Metal Organic Compounds, vols. 1/2, Am. Chem. Soc., Washington, DC, 1965.
[24] G. Åkerlöf, H.E. Turck, J. Am. Chem. Soc. 57 (1935) 1746–1750.
[25] J.D. Floyd, P.M. Gross Jr., J. Am. Chem. Soc. 77 (1955) 1435–1437.
[26] A.T. Kan, G. Fu, M.B. Tomson, Ind. Eng. Chem. Res. 42 (2003) 2399–2408.
[27] K.A. Kraus, R.J. Raridon, W.H. Baldwin, J. Am. Chem. Soc. 86 (1964) 2571–2576.
[28] W.H. Baldwin, R.J. Raridon, K.A. Kraus, J. Phys. Chem. 73 (1969) 3417–3420.
[29] R. Masoudi, B. Tohidi, R. Anderson, R.W. Burgass, J. Yang, Fluid Phase Equilib. 219 (2004) 157–163.